# Preagostic Rh−H Interactions and C−H Bond Functionalization: A Combined Experimental and Theoretical Investigation of Rhodium(I) Phosphinite Complexes

Jared C. Lewis,† Jessica Wu,† Robert G. Bergman,*,†,‡ and Jonathan A. Ellman*,†

*Department of Chemistry, University of California, Berkeley, and the Division of Chemical Sciences, Lawrence Berkeley National Laboratory, Berkeley, California 94720*

*Received August 12, 2005*

Three Rh−phosphinite complexes with the general structural formula $[RhCl(i\text{-}Pr_2POXy)(L)]_2$ (Xy = 2,3-xylyl; L = $PPh_3$, $PMe_3$, *t*-BuNC) were synthesized. Characterization of these complexes using crystallographic and spectroscopic techniques revealed rare examples of preagostic C−H···M interactions. $^1H$ NMR chemical shielding calculations on a geometry-optimized model complex were used to provide a connection between the solution and solid-state data, which additionally supported assignment of the preagostic interaction. One of these Rh−phosphinite complexes (L = $PPh_3$) was used to catalyze the ortho alkylation of phosphinites and phenols with an unactivated alkene. Finally, DFT calculations were used to provide evidence for the involvement of the observed preagostic interaction in the cyclometalation step of the catalytic cycle.

## Introduction

Catalytic methods for selective activation and subsequent functionalization of carbon−hydrogen (C−H) bonds provide an atom-economical alternative to conventional procedures using halogenated or metalated starting materials.[1] However, exceptionally demanding requirements are placed on such systems. A potential catalyst must activate a relatively inert C−H bond in the presence of other diverse functional groups, efficiently functionalize the metalated carbon, and discriminate between the various C−H bonds in a molecule to provide the desired product.

Despite these stringent requirements, a number of transformations proceeding via C−H bond activation have been developed.[2] These methods generally rely on the use of functional-group-tolerant late metals (groups 8−10 in particular) with ligands capable of stabilizing a reactive metal fragment. The challenge of regioselectivity has been met either by taking advantage of steric interaction between substrate and catalyst to force the catalyst to the most accessible C−H bond or,[3] more commonly, by using heteroatom coordination to direct the catalyst to a site proximal to the C−H bond to be functionalized.[4]

Bedford and co-workers have applied the latter method in their novel protocol for the ortho arylation of phenols.[5] This process involves the use of a Rh catalyst and a catalytic amount of phosphinite to generate a different, but more reactive, phosphinite from a phenol. Once formed, this reactive phosphinite presumably coordinates to the metal catalyst and undergoes cyclometalation, which then allows for selective ortho arylation by a standard cross-coupling mechanism. Transfer of the $PR_2$ group to another molecule of phenol releases

* To whom correspondence should be addressed. E-mail: bergman@cchem.berkeley.edu (R.G.B.); jellman@uclink.berkeley.edu (J.A.E.).

† Department of Chemistry, University of California.

‡ Division of Chemical Sciences, Lawrence Berkeley National Laboratory, University of California.

(1) For reviews focusing on C−H bond activation with discussions on the challenges of functionalization, see: (a) Crabtree, R. H. *Chem. Rev.* **1985**, *85*, 245. (b) Arndsten, B. A.; Bergman, R. G.; Mobley, T. A.; Peterson, T. H. *Acc. Chem. Res.* **1995**, *28*, 154−162. (c) Shilov, A. E.; Shul'pin, G. B. *Chem. Rev.* **1997**, *97*, 2879. (d) Crabtree, R. H. *Dalton Trans.* **2001**, 2437−2450. (e) Bercaw, J. E.; Labinger, J. A. *Nature* **2002**, *417*, 507−514.

(2) For reviews of methods involving catalytic C−H functionalization see: (a) Dyker, G. *Chem. Ber.* **1997**, *130*, 1567−1578. (b) Dyker, G. *Angew. Chem., Int. Ed.* **1999**, *38*, 1698−1712. (c) Miura, M.; Nomura, M. *Top. Curr. Chem.* **2002**, *219*, 212−237. (d) Kakiuchi, F.; Murai, S. *Acc. Chem. Res.* **2002**, *35*, 826−834. (e) Jia, C.; Kitamura, T.; Fujiwara, Y. *Acc. Chem. Res.* **2001**, *34*, 633−634. (f) Guari, Y.; Sabo-Etienne, S.; Chaudret, B. *Eur. J. Inorg. Chem.* **1999**, 1047−1055. (g) Kakiuchi, F.; Chatani, N. *Adv. Synth. Catal.* **2003**, *345*, 1077−1101. (h) Kakiuchi, F.; Murai, S. *Top. Curr. Chem.* **1999**, *3*, 47−77.

(3) For examples of methods utilizing steric factors to affect regioselectivity of C−H bond functionalization: (a) Chen, H.; Schlecht, S.; Semple, T. C.; Hartwig, J. F. *Science* **2000**, *287*, 1995. (b) Cho, J.-Y.; Iverson, C. N.; Smith, M. R. *J. Am. Chem. Soc.* **2000**, *122*, 12868. (c) Ishiyama, T.; Takagi, J.; Kousaku, I.; Miyaura, N.; Anastasi, N. R.; Hartwig, J. F. *J. Am. Chem. Soc.* **2001**, *124*, 390.

(4) Two distinct mechanisms for heteroatom-directed C−H functionalization have been noted. One mechanism involves selective activation of a C−H bond proximal to a directing group by a coordinated metal fragment followed by functionalization of the metalated carbon: (a) Kakiuchi, F.; Sekine, S.; Tanaka, Y.; Kamatini, A.; Sonoda, M.; Chatani, N.; Murai, S. *Bull. Chem. Soc. Jpn.* **1995**, *68*, 62−83. The second involves reversible C−H activation of many sites in a molecule by a metal fragment with functionalization occurring only proximal to a directing group: (b) Lenges, C. P.; Brookhart, M. *J. Am. Chem. Soc.* **1999**, *121*, 6616−6623. For recent examples of methods utilizing heteroatom directed C−H functionalization see: (c) Kametani, Y.; Satoh, T.; Miura, M.; Nomura, M. *Tetrahedron Lett.* **2000**, *41*, 2655−2658. (d) Oi, S.; Fukita, S.; Hirata, N.; Watanuki, N.; Miyano, S.; Inoue, Y. *Org. Lett.* **2001**, *3*, 2579−2581. (e) Oi, S.; Ogino, Y.; Fukita, S.; Inoue, Y. *Org. Lett.* **2002**, *4*, 1783−1785. (f) Kakiuchi, F.; Murai, S. *Acc. Chem. Res.* **2002**, *35*, 826−834. (g) Tan, K. L.; Park, S.; Ellman, J. A.; Bergman, R. G. *J. Org. Chem.* **2004**, *69*, 7329−7335. (h) Thalji, R. K.; Ellman, J. A.; Bergman, R. G. *J. Am. Chem. Soc.* **2004**, *126*, 7192−7193. (i) Lewis, J. C.; Wiedemann, S. H.; Bergman, R. G.; Ellman, J. A.; *Org. Lett.* **2004**, *6*, 35−38.

(5) (a) Bedford, R. B.; Coles, S. J.; Hursthouse, M. B.; Limmert, M. E. *Angew. Chem., Int. Ed.* **2003**, *42*, 112−114. (b) Bedford, R. B.; Limmert, M. E. *J. Org. Chem.* **2003**, *68*, 8669−8682.

(6) Taken from ref 5b.

10.1021/om050700i CCC: $30.25 
Publication on Web 10/11/2005

**Scheme 1**[6]

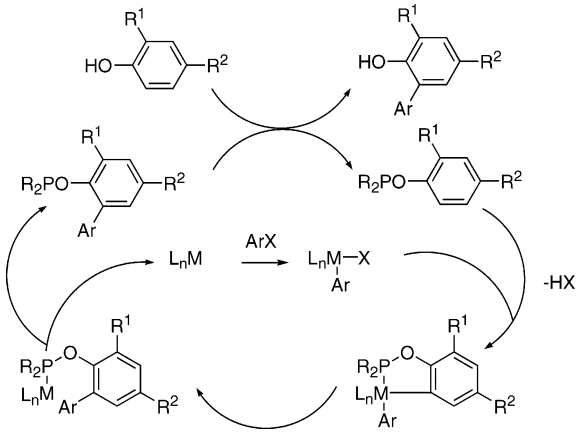


the desired product and regenerates another 1 equiv of the reactive phosphinite to complete the catalytic cycle (Scheme 1). We became interested in using the metallacycle intermediate proposed in this mechanism for different types of transformations such as hydroarylation.[2d] A detailed study of Rh(I) phosphinite complexes was therefore undertaken in order to better understand the behavior of these species.

We disclose here the synthesis of three non-cyclometalated rhodium−phosphinite complexes, which were found to exhibit rare examples of preagostic interactions between the rhodium centers and the hydrogen ortho to the oxygen of the phosphinite ligands. Such an interaction is of interest due to both its possible implications for the mechanism of C−H activation and functionalization reactions and the general lack of characterization of such complexes involving $d^8$ transition metals in the literature. A number of experimental and computational techniques were used to characterize this interaction. One of the complexes underwent stoichiometric C−H bond activation and subsequent alkylation ortho to the phosphinite directing group. The use of these systems for catalytic alkylation of phenols in both an inter- and intramolecular fashion was then investigated. Finally, a mechanism for the C−H activation reaction occurring during these transformations is proposed on the basis of density functional theory (DFT) calculations.

## Results and Discussion

**Synthesis and Characterization of Rh−Phosphinite Complexes.** Complexes **2a**−**c** were prepared by heating toluene solutions of $[RhCl(coe)_2]_2$ (coe = cyclooctene), phosphinite **1a**, and the appropriate ligand, L (Scheme 2).

High conversions of **1a** to the corresponding rhodium complexes were observed by $^1H$ and $^{31}P$ NMR spectroscopy. Vapor diffusion of pentane into toluene solutions of the reaction mixtures provided analytically pure products in good yields after filtration (**2a**, 73%; **2b**, 65%; **2c**, 72%). Analysis of the $^1H$ NMR spectra of complexes **2a**−**c** revealed significantly downfield shifted resonances corresponding to the protons ortho ($H_a$) to the phosphinite oxygens (Table 1). A nondecoupled 1-D HMQC NMR spectroscopic analysis of **1a** and **2c** revealed only a minor increase in $^1J_{C-H}$ for the ortho carbon ($C_a$) of the free (159.5 Hz) and bound (162.3 Hz)

**Scheme 2**

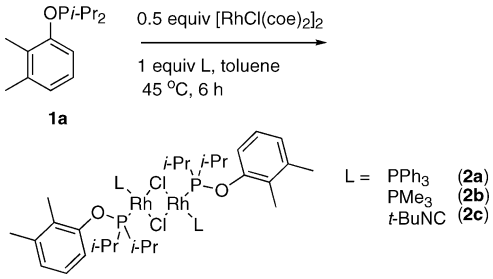


**Table 1. Comparison of NMR Data for $H_a$ in 1a and 2a−c**

| | 1a | 2a | 2b | 2c |
|---|---|---|---|---|
| $\delta$ (ppm) | 7.11 | 10.30 | 9.51 | 9.25 |
| $\Delta\delta$ (ppm) | - | 3.19 | 2.40 | 2.14 |
| splitting | dd | d | d | d |
| $J$ (Hz) | 8.4, 3.7 | 8.2 | 8.2 | 8.3 |

phosphinite ligands, and no Rh−H coupling was observed for any of the complexes. Although these initial data did not indicate the presence of a formal agostic interaction, it still seemed likely that the anomalous chemical shifts of the protons of the phosphinite ligands were cause by some type of coordination to the nearby Rh atom. We decided to further investigate this interaction, due to its possible implications for subsequent reactions of this C−H bond.

Crystals of complexes **2a**−**c** were obtained by vapor diffusion of pentane into toluene solutions at room temperature. X-ray analysis provided the dimeric structures shown in Figures 1−3 for complexes **2a**−**c**, respectively. The coordination geometry around each rhodium is essentially square planar with deviations in the angles of no more than 10° and no unusual Rh−L or Rh−Cl bond lengths. The fold angle ($\lambda$) between the two square planes comprising the dimers varies significantly in **2a**−**c**, as has been noted in many other $[L_2RhCl]_2$ structures.[7]

Further examination of these structures also revealed a relatively short interatomic distance between $H_a$ of the phosphinite ligand and the rhodium center (H15 and H53, H1 and H1_2, and H24 and H56 in Figures 1−3, respectively). The Rh···$H_a$ distances and the $C_a$−$H_a$···Rh angles of the three complexes ranged from 2.77 to 3.01 Å and from 136 to 141°, respectively (Table 3). These observations supported our original hypothesis regarding the involvement of the Rh center in the aforementioned downfield chemical shift perturbations of the ortho protons of the phosphinite ligands of **2a**−**c**; however, full characterization of this interaction still needed to be completed.

A number of metal−hydrogen interactions (X−H···M, X = C, N), including agostic interactions,[8] preagostic

(7) For discussions of fold angles in $[L_2RhCl]_2$ complexes see: (a) Wang, K.; Goldman, M. E.; Emge, T. J.; Goldman, A. S. *J. Organomet. Chem.* **1996**, *518*, 55. (b) Schnabel, R. C.; Roddick, D. M. *Inorg. Chem.* **1993**, *32*, 1513. (c) Curtin, M. D.; Butler, W. M.; Greene, J. *Inorg. Chem.* **1978**, *17*, 2928. (d) Ibers, J. A.; Snyder, R. G. *Acta Crystallogr.* **1962**, *15*, 923. (e) Dahl, L. F.; Martell, C.; Wampler, D. L. *J. Am. Chem. Soc.* **1961**, *83*, 1761.

(8) (a) Brookhart, M.; Green, M. L. H. *J. Organomet. Chem.* **1983**, *250*, 395. (b) Brookhart, M.; Green, M. L. H. *Prog. Inorg. Chem.* **1988**, *36*, 1. (c) Crabtree, R. H.; Hamilton, D. G. *Adv. Organomet. Chem.* **1988**, *36*, 1. (d) Crabtree, R. H. *Angew. Chem., Int. Ed. Engl.* **1993**, *32*, 789. (e) Hall, C.; Perutz, R. N. *Chem. Rev.* **1996**, *96*, 3125.

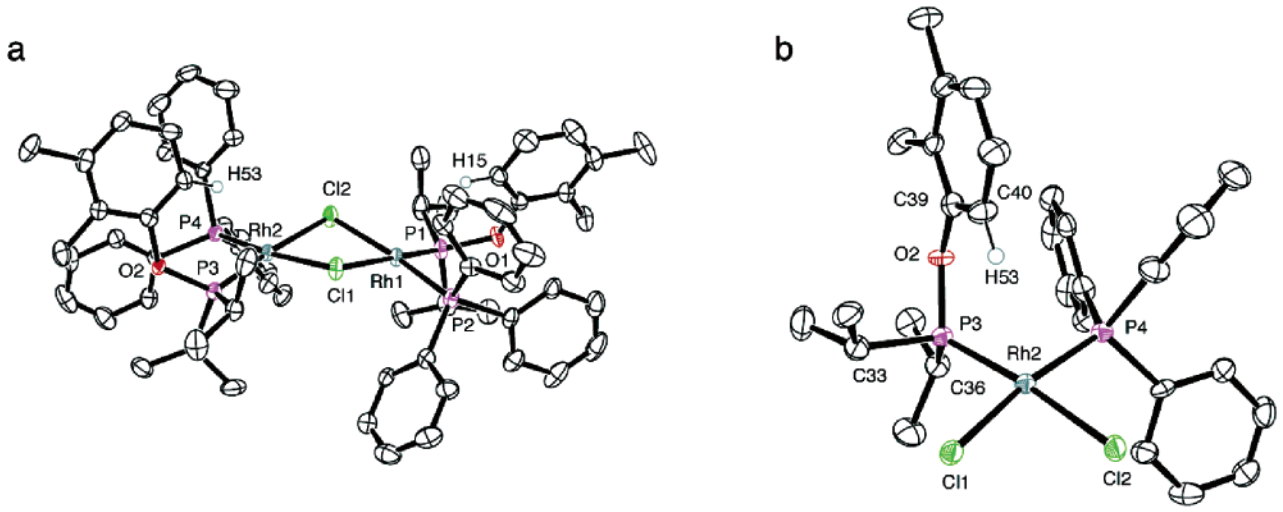


**Figure 1.** ORTEP drawings of (a) the complete dimer structure of **2a** and (b) one of the two Rh centers. Hydrogen atoms distant from the metal center and solvent atoms have been omitted for clarity. Thermal ellipsoids are shown at the 50% probability level.

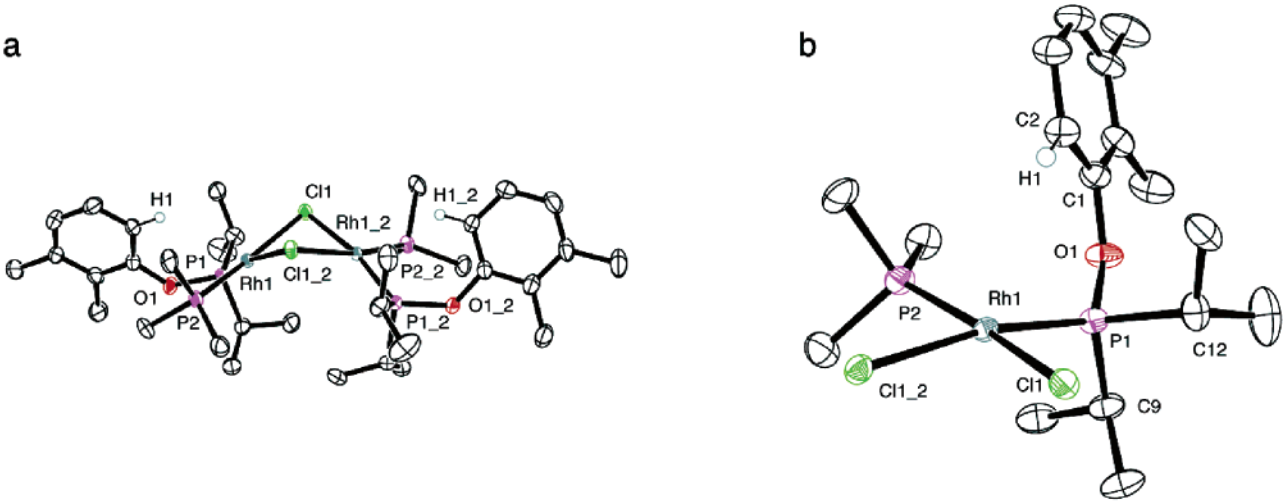


**Figure 2.** ORTEP drawings of (a) the complete dimer structure of **2b** and (b) one of the two Rh centers. Hydrogen atoms distant from the metal center have been omitted for clarity. Thermal ellipsoids are shown at the 50% probability level.

interactions,[9] and hydrogen bonding,[10] have been described in the literature (vide infra). While the divisions between these types of interactions are not absolute, each has signature spectroscopic and geometric properties which allow them to be generally distinguished from one another (Table 4) and from simple metal−hydrogen close contacts.

Agostic interactions are three-center−two-electron bonds in which the electron density of a C−H bond is donated to a metal center.[8a] As a consequence of this interaction, the C−H bond is typically elongated and the C−H···M angle is relatively acute. Agostic interactions exhibit a number of specific NMR characteristics such as upfield shifts in C−H bond proton resonances, M−H coupling for NMR-active metals, and reduction of $^1J_{C-H}$ values for the carbon of the coordinated C−H bond; however, none of these were observed for **2a**−**c**. Linear metal−hydrogen bonds to hydrocarbons, which involve a filled metal d orbital as a hydrogen bond acceptor and a C−H bond as a hydrogen bond donor, represent an extreme in X−H···M geometries opposite to that of agostic interactions.[10] As for traditional hydrogen bonds, a nearly linear arrangement of hydrogen bond donor and acceptor is preferred in order to maximize electrostatic interactions between the hydrogen bond donor and acceptor. Metal−hydrogen bonds have most often been observed with relatively polar N−H bonds, but there has been some discussion of these interactions in C−H···M systems.[10a,b] The C−H···M angles present in **2a**−**c** deviate significantly from 180°, but weak hydrogen bonding cannot be discounted.[9e] Interactions between C−H bonds and metal centers that

(9) (a) Roe, D. M.; Bailey, P. M.; Moseley, K.; Maitlis, P. M. *J. Chem. Soc. Chem. Commun.* **1972**, 1273−1274. (b) Albinati, A.; Anklin, C. G.; Ganazzoli, F.; Rüegg, H.; Pregosin, P. S. *Inorg. Chem.* **1987**, *26*, 503−508. (c) Albinati, A.; Arz, C.; Pregosin, P. S. *Inorg. Chem.* **1987**, *26*, 508−513. (d) Ablinati, A.; Pregosin, P. S.; Wombacher, F. *Inorg. Chem.* **1990**, *29*, 1812−1817. (e) Yao, W.; Eisenstein, O.; Crabtree, R. H. *Inorg. Chim. Acta* **1997**, *254*, 105.

(10) (a) Brammer, L.; Charnock, J. M.; Goggin, P. L.; Goodfellow, R. J.; Koetzle, T. F.; Orpen, A. J. *J. Chem. Soc., Chem. Commun.* **1987**, 443. (b) Brammer, L.; Charnock, J. M.; Goggin, P. L.; Goodfellow, R. J.; Orpen, A. J.; Koetzle, T. F. *J. Chem. Soc., Dalton Trans.* **1991**, 1789. (c) Brammer, L. McCann, M. C.; Bullock, R. M.; McMullan, R. K.; Sherwood, P. *Organometallics* **1992**, *11*, 2339. (d) Lee, J. C.; Rheingold, A. L.; Muller, B.; Pregosin, P. S.; Crabtree, R. H. *J. Chem. Soc., Chem. Commun.* **1994**, 1021. (e) Braga, D.; Grepioni, F.; Tedesco, E. *Organometallics* **1997**, *16*, 1846−1856.

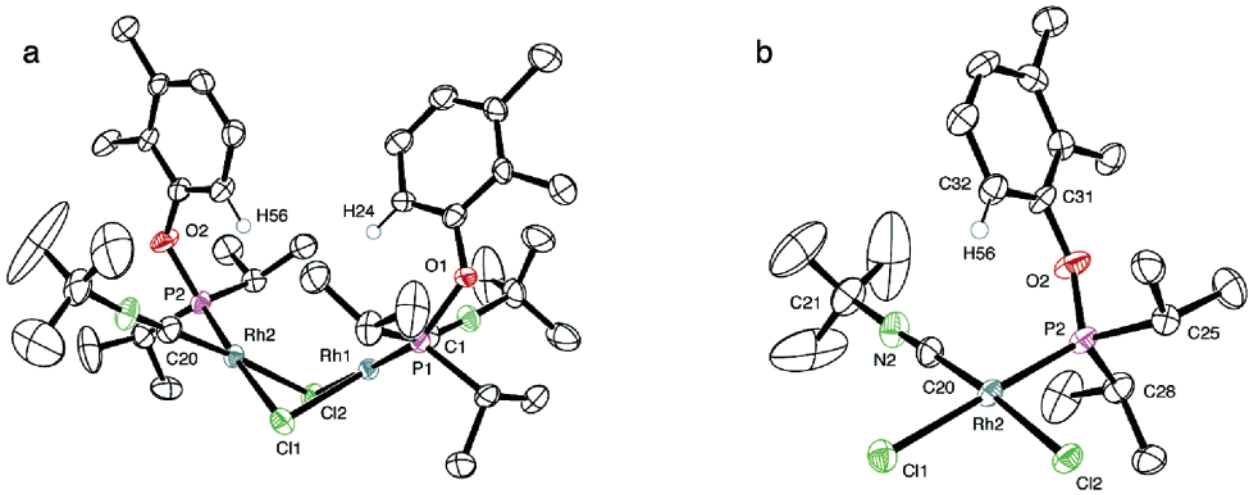


**Figure 3.** ORTEP drawings of (a) the complete dimer structure of **2c** and (b) one of the two Rh centers. Hydrogen atoms distant from the metal center and solvent atoms have been omitted for clarity. Thermal ellipsoids are shown at the 50% probability level.

**Table 2. Crystal Data and Structure Refinement for 2a−c**

| | **2a** | **2b** | **2c** |
|---|---|---|---|
| empirical formula | $Rh_2Cl_2P_4O_2C_{64}H_{76}\cdot C_{3.5}H_4$ | $Rh_2Cl_2P_4O_2C_{34}H_{64}$ | $Rh_2Cl_2P_2O_2N_2C_{38}H_{64}\cdot C_{3.5}H_4$ |
| formula wt | 1323.99 | 905.49 | 965.67 |
| cryst color, habit | yellow, platelike | red, tabular | golden, polyhedral |
| cryst dimens (mm) | 0.10 × 0.07 × 0.27 | 0.06 × 0.10 × 0.16 | 0.14 × 0.25 × 0.29 |
| cryst syst | monoclinic | monoclinic | triclinic |
| lattice type | primitive | *C* centered | primitive |
| lattice params | | | |
| *a*, Å | 12.404(2) | 31.419(3) | 12.854(1) |
| *b*, Å | 30.956(4) | 7.5160(6) | 13.311(2) |
| *c*, Å | 16.505(2) | 17.707(2) | 15.473(2) |
| α, deg | | | 105.193(2) |
| *β*, deg | 90.904(2) | 93.679(1) | 95.559(2) |
| *γ*, deg | | | 111.160(2) |
| *V* (Å$^3$) | 6336(1) | 4172.9(6) | 2328.1(4) |
| space group | $P2_1/c$ (No. 14) | $C2/c$ (No. 15) | $P\bar{1}$ (No. 2) |
| *Z* value | 4 | 4 | 2 |
| $D_{calcd}$ (g/cm$^3$) | 1.388 | 1.441 | 1.377 |
| $F_{000}$ | 2740.00 | 1872.00 | 1002.00 |
| $\mu$(Mo Kα) (cm$^{-1}$) | 7.48 | 10.98 | 9.24 |
| temp (°C) | −133 ± 1 | −113 ± 1 | −144 ± 1 |
| 2$\theta$ range (deg) | 5.00−47.00 | 5.00−49.00 | 5.00−49.00 |
| $2\theta_{max}$ (deg) | 49.4 | 49.5 | 49.4 |
| no. of rflns measd | | | |
| total | 27 984 | 8998 | 11 748 |
| unique | 10 738 | 3713 | 7464 |
| $R_{int}$ | 0.071 | 0.041 | 0.045 |
| *p* factor | 0.0300 | 0.0300 | 0.0300 |
| no. of observns ($I > 3.00\sigma(I)$) | 6428 | 2761 | 5208 |
| no. of variables | 689 | 199 | 464 |
| rfln/param ratio | 9.33 | 13.87 | 11.22 |
| residuals:[a] $R$, $R_w$, $R_{all}$ | 0.044, 0.049, 0.091 | 0.031, 0.039, 0.043 | 0.044, 0.054, 0.069 |
| goodness of fit indicator | 1.34 | 1.34 | 1.31 |

[a] $R = \Sigma||F_o| - |F_c||/\Sigma|F_o|$ and $R_w = [\Sigma w(|F_o| - |F_c|)^2/\Sigma wF_o^2]^{1/2}$, where $w = 1/\sigma^2(F_o)$.

have characteristics between the defined extremes of agostic and hydrogen bonding have been termed remote, pregostic, or preagostic interchangeably.[12] Originally identified by Pregosin and co-workers, these are typified by relatively long M···H distances and large X−H···M angles.[9a−d] Their primary spectroscopic signature is a downfield shift in resonances for protons involved in the interaction.[9e] Coupling of this proton to NMR-active metals as well as changes in $^1J_{C-H}$ are not observed. In comparison to the defining characteristics of agostic, hydrogen-bonding, and preagostic interactions, the geometric parameters observed for **2a−c** best fit the definition of complexes containing a preagostic metal−hydrogen interaction. To gain further insight into this interaction, and to provide a connection between the solution and solid-state data used to characterize **2a−c**, a computational study was undertaken.

**Computational Studies of the Rh···H−C Interaction.** The atomic coordinates for **2a** were used to build

(11) Data taken from ref 9e.

(12) (a) Crabtree, R. H. *Angew. Chem., Int. Ed. Engl.* **1993**, *32*, 789. (b) Bortolin, M.; Bucher, U.; Reugger, H.; Venanzi, L. M.; Albinati, A.; Lianza, F. *Organometallics* **1992**, *11*, 2514. (c) Cano, M.; Heras, J. V.; Maeso, M.; Alvaro, M.; Fernández, R.; Pinilla, E.; Campo, J. A.; Monge, A. *J. Organomet. Chem.* **1997**, *534*, 159. (d) Krumper, J. R.; Gerisch, M.; Magistrato, A.; Rothlisberger, U.; Bergman, R. G.; Tilley, T. D. *J. Am. Chem. Soc.* **2004**, *126*, 12492.

**Table 3. Summary of Interatomic Distances (Å) and Bond Angles (deg) Relevant to Rh···$H_a$ Interactions in 2a−c[a]**

| | 2a | 2b | 2c |
|---|---|---|---|
| Rh···$H_a$ | 2.77 | 3.01 | 2.98 |
| Rh′···$H_a$′[b] | 2.84 | 3.01 | 2.92 |
| Rh···$C_a$ | 3.56 | 3.76 | 3.73 |
| Rh···$C_a$′[b] | 3.61 | 3.76 | 3.69 |
| Rh−$H_a$−$C_a$ | 141.34 | 136.16 | 136.01 |
| Rh−$H_a$′−$C_a$′[b] | 139.25 | 136.16 | 138.91 |
| $\lambda$[c] | 205.5 | 234.9 | 69.7 |

[a] The non-hydrogen atoms were refined anisotropically; hydrogen atoms were included but not refined. Bond length or angle derived from calculated location of $H_a$. [b] The prime symbol refers to data for the second half of the dimer complex. [c] Fold angle between two square planes of the dimeric structure.

**Table 4. Comparison of X−H···M Interactions[11]**

| | Agostic | Preagostic | H-bond | 2a-c |
|---|---|---|---|---|
| |  | 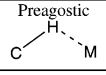 | 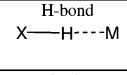 | 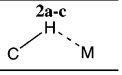 |
| Bonding | 3c-2e | - | 3c-4e | - |
| Δδ | upfield | downfield | downfield | downfield |
| $<_{X-H\cdots M}$ | 90°-130° | 130°-170° | 160°-180° | 136°-141° |
| $d_{M-H}$ | 1.8 - 2.2 Å | 2.3 - 2.9 Å | 2.65-3.5 Å | 2.76-2.98 Å |

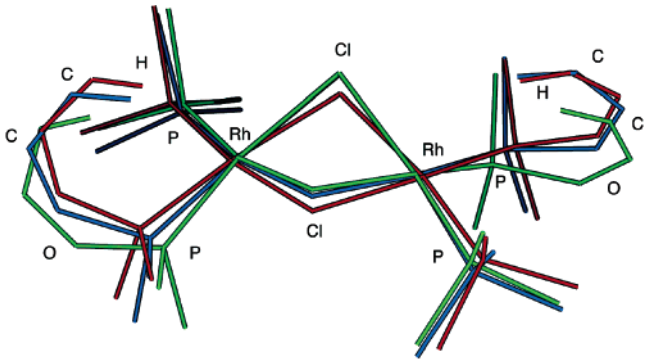


**Figure 4.** Superimposed structures of **2a** (red), **2b** (green), and **3** (blue). Only the structural features common to all structures are included, and portions of the aryl rings are omitted for clarity.

the model compound $[RhCl(PMe_3)(Me_2POXy)]_2$ (**3**), which was geometry optimized in Gaussian03 using DFT calculations at the mPW1PW91/SDD level of theory. The calculated structure ($d_{Rh\cdots H}$ = 2.792, 2.805 Å; $\angle_{C-H\cdots Rh}$ = 137.89, 137.02°; $\lambda$ (fold angle, vide supra) = 231.3°) agreed well with that of **2a** ($d_{Rh\cdots H}$ = 2.765, 2.842 Å; $\angle_{C-H\cdots Rh}$ = 141.34, 139.25°; $\lambda$ = 205.5°) and **2b** ($d_{Rh\cdots H}$ = 2.984, 2.919 Å; $\angle_{C-H\cdots Rh}$ = 136.01, 138.91°; $\lambda$ = 234.9°) (Figure 4). The calculated bond distances of **3** were within 5% of those in **2a**,**b**, except for those of the P−O bonds, which were slightly elongated (7−10%) in the calculated structure.

Importantly, $^1$H NMR chemical shielding calculations indicated that the preagostic, ortho proton of **3** should have a chemical shift of 9.68 ppm. This value agrees well with the chemical shifts observed experimentally for **2a**,**b** at 10.30 and 9.51 ppm, respectively. This result provides further support for the presence of a preagostic interaction in both the solid and solution state by providing a link between the crystal structures and spectroscopic data for **2a**−**c**. Having extensively characterized the preagostic interactions in **2a**−**c**, we next desired to study the reactivity of these complexes.

**Chemistry of Rh−Phosphinite Complexes.** Initial investigations of the reactivity of **2a** focused on attempts to generate cyclometalated phosphinite species from this complex, since such intermediates were proposed by Bedford and coworkers in their studies on the ortho arylation of phenols using Rh−phosphinite mixtures.[13] However, no significant change in the observed chemical shift for the ortho proton of the phosphinite ligand of **2a** was observed by in situ NMR spectroscopy experiments in $d_8$-toluene or $d_8$-THF at room temperature. Thermolysis of **2a** in $d_8$-toluene did not result in reaction until decomposition occurred at temperatures ranging from 45 to 135 °C, and attempts to intercept any intermediate hydridic species as the corresponding chloride by exchange with $CCl_4$ met with no success.[14]

Although synthesis of cyclometalated products was not successful, it was observed that addition of 2 equiv of $PPh_3$ to a solution of **2a** in toluene provided the bis(phosphine)−phosphinite complex *cis*-$RhCl(PPh_3)_2$-(*i*-$Pr_2POXy$) (**4a**) (Scheme 3). In situ $^1$H NMR spectroscopy revealed that the characteristic downfield doublet for the ortho proton of the phosphinite ligand in **2a** had shifted significantly upfield to 9.07 ppm. The $^{31}P\{^1H\}$ NMR spectrum of **4a** showed three major signals at 153.3 ppm (ddd, $^1J_{Rh-P1a}$ = 163.4 Hz, $^2J_{P1a-PPh_3,trans}$ = 368.6 Hz, $^2J_{P1a-PPh_3,cis}$ = 36.7 Hz), 49.4 ppm (dt, $^1J_{Rh-P,P}$ = 195.8 Hz, $^2J_{P-PPh_3/1a}$ = 36.5 Hz), and 27.5 ppm (ddd, $^1J_{Rh-P1a}$ = 163.4 Hz, $^2J_{P1a-PPh_3,trans}$ = 368.6 Hz, $^2J_{P1a-PPh_3,cis}$ = 36.7 Hz). The relatively large $^2J_{P-P}$ coupling constant indicated a trans relationship between Rh-bound **1a** and one of the $PPh_3$ ligands, while the smaller $^2J_{P-P}$ coupling constant was consistent with a cis relationship between the remaining $PPh_3$, Rh-bound **1a**, and the $PPh_3$ ligand trans to **1a**.[15] It was also found that heating a $d_8$-toluene solution of **2a** and neohexene provided the alkylated ligand in 17% yield (Scheme 3).[16] Addition of 2 equiv of $PPh_3$ or **1a** to this reaction mixture provided the same alkylated product in 35% and 67% yields, respectively. These results indicated that a bis(phosphine)−phosphinite or phosphine−bis(phosphinite) complex might be involved in the alkylation reaction.

Alkylation of **1a** with neohexene was also attempted in a catalytic fashion, in analogy to the work by Bedford and coworkers (vide supra).[5] It was found that heating $d_8$-toluene solutions of 2,3-dimethylphenol, neohexene, and **2a** provided the desired products in 31% yield (Scheme 4; Table 5, entry 1). In analogy to the stoichiometric reaction, acceleration of the alkylation in the presence of $PPh_3$ implicated a bis(phosphine) complex

(13) (a) Parshall, G. W. *Acc. Chem. Res.* **1970**, *3*, 139. (b) Dehand, J.; Pfeffer, M. *Coord. Chem. Rev.* **1976**, *18*, 327. (b) Bruce, M. I. *Angew. Chem., Int. Ed.* **1977**, *16*, 73. (c) Omae, I. *Chem. Rev.* **1979**, *79*, 287. (d) Rothwell, I. P. *Acc. Chem. Res.* **1988**, *21*, 153. (e) Newkome, G. R.; Puckett, W. E.; Gupta, V. K.; Kiefer, G. E.; *Chem. Rev.* **1986**, *86*, 451.

(14) Crabtree, R. H. Metal Alkyls, Aryls, and Hydrides and Related σ-bonded Ligands. In *The Organometallic Chemistry of the Transition Metals*, 3rd ed.; Wiley: New York, 2001; p 70.

(15) Similarly large $^2J_{P-P}$ coupling has been observed in rhodium(I) complexes with trans phosphinites: (a) Feiken, N.; Pregosin, P.; Trabesinger, B. *Organometallics* **1998**, *17*, 4510−4518. (b) Irvine, D. J.; Cole-Hamilton, D. J.; Barnes, J.; Hodgson, P. K. G. *Polyhedron* **1989**, *8*, 1575−1577.

(16) Stoichiometric alkylation of cyclometalated Ru−phosphinite complexes has been accomplished: Parshall, G. W.; Knoth, W. H.; Schunn, R. A. *J. Am. Chem. Soc.* **1969**, *91*, 4990−4995. Catalytic alkenylation of phenols has been accomplished: Nishinaka, Y.; Satoh, T.; Miura, M.; Morisaka, H.; Nomura, M.; Matsui, H.; Yamaguchi, C. *Bull. Chem. Soc. Japn.* **2001**, *74*, 1727−1735. Catalytic alkylation of phenols has been accomplished using norbornene (Dorta, R.; Togni, A. *Chem. Commun.* **2003**, 760−761) and ethylene (Lewis, L. N.; Smith, J. F. *J. Am. Chem. Soc.* **1986**, *108*, 2728−2735).

**Scheme 3**

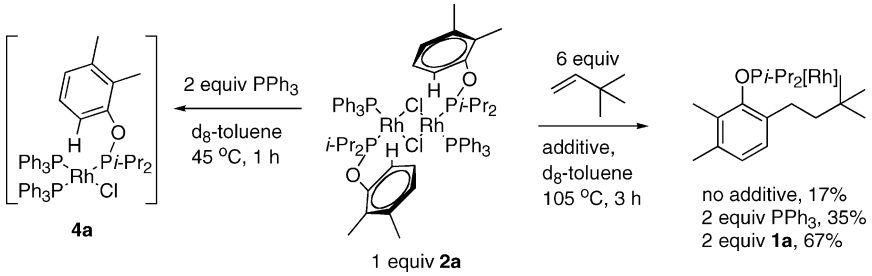


**Scheme 4**

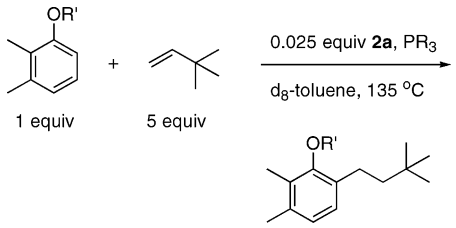


**Scheme 5**

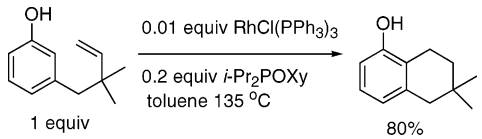


**Table 5. Effects of Added Phosphine/Phosphinite Additives on Alkylation of 1a[a]**

| | | | amt of $PR_3$ | alkylation (%) | | |
|---|---|---|---|---|---|---|
| reacn | R′ | $PR_3$ | (equiv) | 2.8 h | 5.5 h | 24 h |
| 1 | H | | 0 | 22 | 26 | 31 |
| 2 | H | $PPh_3$ | 0.1 | 59 | 69 | 83 |
| 3 | H | *i*-$Pr_2POXy$ | 0.1 | 88 | 96 | 98 |
| 4 | P-*i*-$Pr_2$ | | 0 | 95 | 100 | |
| 5 | P-*i*-$Pr_2$ | $PPh_3$ | 0.1 | 92 | 92 | |

[a] Yields determined by $^1H$ NMR spectroscopy relative to dimethoxytoluene internal standard.

as the active catalyst (entry 2). Further rate acceleration was observed using a phosphinite cocatalyst, as shown in Table 5 (entry 3), and nearly quantitive alkylation was obtained under these conditions. No reaction was observed in the absence of phosphinite ligand, and no increases in conversion were observed upon addition of triethylamine (to facilitate phosphinite catalyst turnover) to the reaction mixture. Alkylation occurred exclusively at the ortho position of the phenol. It was also found that heating a $d_8$-toluene solution of **1a** and a catalytic amount of **2a** under 1 atm of $D_2$ led to 75% incorporation of D at the ortho position and no measurable incorporation of D at the meta or para position of 2,3-dimethylphenol following acidic workup of the reaction mixture. Presumably, the rate acceleration associated with the addition of phosphinite ligand in the catalytic reaction, as well as the increased conversion observed with the addition of phosphinite ligand in the stoichiometric reaction, indicated that the phosphinite served both as a ligand and as a substrate for alkylation.

While **2a** is an efficient catalyst for the ortho alkylation of 2,3-dimethylphenol, this complex is not ideal for the alkylation of other phenols, due to the generation of alkylated **1a** from the initial turnover of **2a**. Furthermore, **2a** is not commercially available, which limits possible application of this chemistry. We therefore established a simple alkylation protocol utilizing Wilkinson's catalyst as an inexpensive, commercially available catalyst precursor and (2,6-xylyl)diisopropylphosphinite (**1b**) as a phosphinite ligand. Phosphinite **1b**, which has its ortho positions blocked with methyl groups, allowed use of this species as a cocatalyst for the ortho alkylation. Specifically, 2,3-dimethylphenol, neohexene, Wilkinson's catalyst, and **1b** were refluxed at 135 °C for 6 h to provide the alkylated phenol in 72% isolated yield.

An intramolecular variant of the olefin coupling was also explored (Scheme 5). In this case, the substrate, Wilkinson's catalyst, and **1b** were refluxed in toluene to provide quantitative conversion to the desired product (80% isolated yield). A number of substrates bearing tethers of varying olefin substitution, length, and heteroatom constitution were submitted to these reaction conditions, but either olefin isomerization or no reaction occurred in each case. Despite the limited substrate scope of these reactions, the aforementioned successes represent a useful extension of Bedford's arylation method for alkylation of phenols.

**Proposed Reaction Pathway.** We finally wished to establish a link between the preagostic interaction observed in the catalysts (**2a** and **4a**) and the oxidative addition step of the catalytic cycle for the alkylation reaction. The importance of inter- and intramolecular C−H bond activation by metal complexes has led to a number of investigations into the individual intermediates and dynamics of these transformations.[17] In particular, Crabtree and co-workers studied a collection of compounds exhibiting a range of C−H···M interactions in order to model the approach of C−H bonds to a metal center using the static structure method of Bürgi and Dunitz.[18] Their analysis focused on the effective covalent radius for C−H bonding electrons ($r_{bp}$) and provided evidence that C−H oxidative addition begins with a weak interaction between a C−H bond and a metal center ($r_{bp} > 1.0$ Å) and proceeds through geometries typical of agostic intermediates (0.7 Å $< r_{bp} <$ 1.0 Å) to provide the final product ($r_{bp} < 0.7$ Å) (Figure 5).

Bedford and co-workers proposed that C−H bond activation of a phosphinite generated in situ during their method for ortho arylation of phenols occurs to give a metallacycle intermediate. Cyclometalation of phosphinite ligands by a variety of metals has been ob-

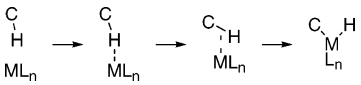


**Figure 5.** General coordinate for oxidative addition of C−H bonds.

**Scheme 6. Proposed Reaction Pathway for Cyclometalation**

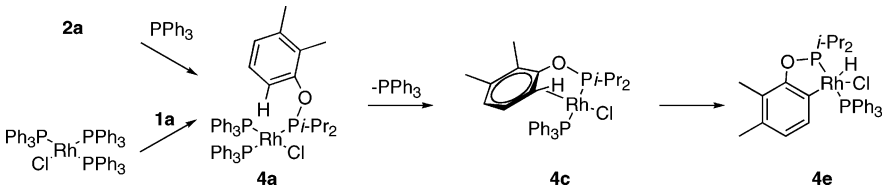


served,[19] but it is well-known that cyclometalated intermediates are not necessarily isolable, despite apparently favorable geometric and electronic factors.[13] Although no cyclometalated products were observed in our alkylation studies or in the arylation chemistry developed by Bedford, both investigations provided strong evidence for the intermediacy of a cyclometalated species produced by C−H bond activation of the phosphinite ligand. The correlations that we observed between preagostic interactions that were identified for complexes **2a**−**c** and the catalytic activity of **2a** in the ortho alkylation reaction of 2,3-dimethylphenol prompted our investigation into the mechanism for the cyclometalation of phosphinite ligands using Crabtree's analysis of C−H bond oxidative addition as a guide for the geometries of intermediates along the proposed pathway.

The observed formation of *cis*-$RhCl(PPh_3)_2(i\text{-}Pr_2POXy)$ from both **2a**/$PPh_3$ and Wilkinson's catalyst/**1a,** and the increased catalytic activity of these complexes relative to **2a** alone, implicated this species as the resting state for the alkylation catalyst.[20] We therefore envisioned formation of a bis(phosphine) intermediate, **4a**, from dimer fragmentation and addition of $PPh_3$ to **2a** (Scheme 6). In catalytic reactions involving Wilkinson's catalysts, this step corresponds to a ligand exchange of $PPh_3$ for **1a**. Displacement of phosphine by the incoming C−H bond could give rise to the agostic intermediate **4c**, which following C−H activation would give the product **4e**.

DFT calculations (B3LYP, LACVP**++) were used to model the reaction coordinate for the C−H activation pathway proposed in Scheme 6 using $Me_2POPh$ and $PMe_3$ in place of **1a** and $PPh_3$, respectively. All intermediates were confirmed by frequency calculations (all positive frequencies observed for intermediates and a single imaginary frequency observed for transition states), and the vibration associated with each imaginary frequency was observed to be consistent with the proposed transformation. The pathways for both *cis*- and *trans*-bis(phosphine) complexes were modeled in order to identify any major differences in the reactivity of the two isomers.

Calculations commenced with a geometry optimization of complex **5a**, which has structural parameters

**Table 6. Selected Energies, Distances, and Angles for *cis*- and *trans*-5a−e**

| complex | $\Delta G$ (kcal/mol) | $d_{C-H}$ (Å) | $d_{Rh-C}$ (Å) | $d_{Rh-H}$ (Å) | C−H···Rh (deg) | $r_{bp}$ (Å) |
|---|---|---|---|---|---|---|
| *cis*-**5a** | 0 | 1.085 | 3.859 | 3.027 | 133.87 | 1.9 |
| *cis*-**5b** | 34.1 | 1.153 | 2.393 | 1.847 | 103.4 | 0.6 |
| *cis*-**5c** | 13.2 | 1.174 | 2.274 | 1.765 | 99.4 | 0.5 |
| *cis*-**5d** | 19.7 | 1.532 | 2.102 | 1.595 | 84.5 | 0.3 |
| *cis*-**5e** | 10.7 | 2.318 | 2.054 | 1.517 | 60.6 | 0.0 |
| *trans*-**5a** | −3.2 | 1.087 | 3.641 | 2.770 | 137.0 | 1.6 |
| *trans*-**5b** | 18.6 | 1.106 | 2.709 | 2.077 | 113.1 | 0.9 |
| *trans*-**5c** | 8.1 | 1.114 | 2.502 | 2.000 | 103.2 | 0.7 |
| *trans*-**5d** | 20.1 | 1.664 | 2.103 | 1.558 | 81.4 | 0.2 |
| *trans*-**5e** | 14.6 | 2.508 | 2.082 | 1.513 | 56.0 | −0.1 |

analogous to those of complex **4a** (Table 6). The Rh···H bond lengths, C−H···M angles, and effective covalent radius ($r_{bp}$, vide supra) value (1.9) of complex **5a** are consistent with a preagostic interaction. While *cis*-**4a** was observed by NMR spectroscopy, *trans*-**5a** was calculated to be more stable than *cis*-**5a** by 3.2 kcal/mol. This small discrepancy could be a result of the simplifications made to **4a** present in **5a**. Transition state **5b** involves the loss of a phosphine ligand and was minimized next. A number of attempts to minimize pentacoordinate bis(phosphine) structures provided either **5a** or **5c**, presumably due to the steric congestion about the Rh center for these complexes. The calculated energetic barrier leading from the trans isomer of **5a** to transition state **5b** is 21.8 kcal/mol; it is 34.1 kcal/mol for the cis isomer. These values are consistent with experimental and calculated values for phosphine dissociation from late-metal complexes.[21] A relatively large difference in energy (15.5 kcal/mol) between the cis and trans complexes (**5b**) was calculated, indicating that the cyclometalation may actually proceed through the trans pathway, but additional experimental evidence is needed to confirm this. The Rh−C/H bond distances, C−H···Rh angles, and $r_{bp}$ values (0.5 and 0.7 Å) calculated for *cis*- and *trans*-**5c** agreed well with literature examples of agostic interactions.

Next, the oxidative addition transition state **5d** was located. The barrier for C−H activation for the trans complex was calculated to be 12.0 kcal/mol and only 6.5 kcal/mol in the cis complex, which is consistent with literature reports of low energetic barriers for cyclometalation of ligands on $d^8$ metal−phosphine complexes. Finally, the cyclometalated structures, **5e**, were minimized and found to be about 15 kcal/mol higher in energy than the preagostic complexes **4a**; this energy difference may explain our inability to observe or isolate any cyclometalated products. These calculations are consistent with the involvement of the preagostic interaction observed in **2a** along the proposed path for cyclometalation of this complex (Figure 6).

(17) For computational studies see: (a) Saillard, J.-Y.; Hoffmann, R. *J. Am. Chem. Soc.* **1984**, *106*, 2006. (b) Cundari, T. R. *J. Am. Chem. Soc.* **1994**, *116*, 340. (c) Koga, N.; Morokuma, K. *Chem. Rev.* **1991**, *91*, 823. For experimental studies, see: (d) ref i. (e) Ryabov, A. D. *Chem. Rev.* **1990**, *90*, 403.

(18) Crabtree, R. H.; Holt, E. M.; Lavin, M.; Morehouse, S. M. *Inorg. Chem.* **1985**, *24*, 1986.

(19) Bedford, R. B.; Hazelwood, S. L.; Horton, P. N.; Hursthouse, M. B. *Dalton Trans.* **2003**, 4164.

(20) When $PPh_3$ was replaced with **1a** or **1b** as both the ligand and the substrate, a bis(phosphinite) species, $RhCl(PPh_3)(i\text{-}Pr_2POXy)_2$, could also serve as the active catalyst; however, $PMe_3$ should still serve as a useful model for computational studies.

(21) Schmid, R.; Herrmann, W. A.; Frenking, G. *Organometallics* **1997**, *16*, 701.

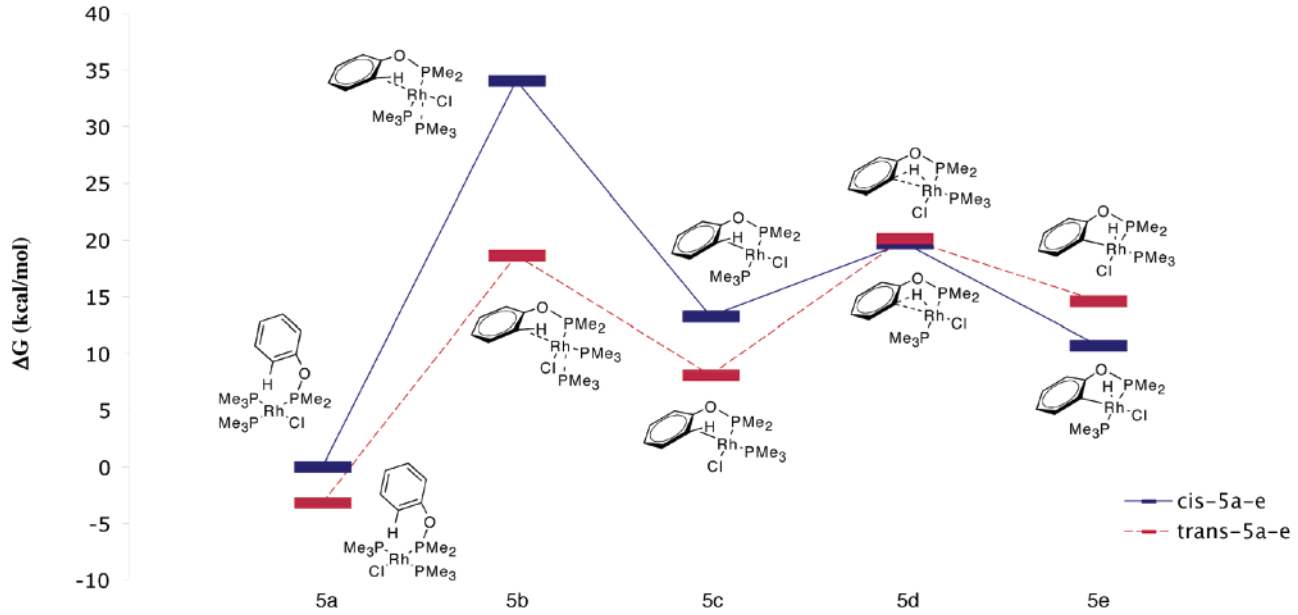


**Figure 6.** Calculated reaction pathway for cyclometalation.

## Conclusion

The results presented in this work have supplied evidence for the involvement of a preagostic interaction in a C−H activation reaction. We have synthesized three Rh−phosphinite complexes which exhibit a rare preagostic interaction. We characterized these complexes using crystallographic and spectroscopic techniques as described for previous examples of preagostic interactions. In addition, we established a connection between solution and solid-state data obtained for these structures using DFT calculations to correlate molecular structure with observed spectroscopic data. We next showed that complex **2a** catalyzes the ortho alkylation of phosphinites and developed a catalytic method for ortho alkylation of phenols with an unactivated alkene. Finally, we used DFT calculations to provide evidence for the involvement of complexes containing a preagostic interaction in the reaction coordinate for cyclometalation of phosphinite ligands.

## Experimental Section

**General Procedures.** All reagents were degassed and handled under an inert nitrogen atmosphere using syringe and cannula techniques. Unless otherwise noted, all organic preparations were carried out in flame- or oven-dried glassware and all organometallic procedures were conducted in a nitrogen-filled Vacuum Atmospheres inert-atmosphere box. Flash column chromatography was carried out using Merck 60 230−400 mesh silica gel. NMR spectra ($^1$H, $^{13}$C, and $^{31}$P) were obtained on a Bruker AMX-400 spectrometer at room temperature. Chemical shifts are reported in ppm, and coupling constants are reported in Hz. $^1$H resonances are referenced to residual protonated solvent, while $^{31}$P resonances are referenced to a trimethyl phosphate external standard. Mass spectrometry was performed by the University of California, Berkeley, mass spectrometry facility or by the aforementioned GC/MS system. X-ray crystal structures were obtained by Drs. Frederick J. Hollander and Allan G. Oliver at the University of California, Berkeley (UCB), X-ray facility (CHEXRAY). Elemental analyses were performed at the UCB Microanalytical facility on a Perkin-Elmer 2400 Series II CHNO/S analyzer.

**Materials.** Unless otherwise noted, all reagents were obtained from commercial suppliers and used without further purification. Molecular sieves (3 Å) were heated at 300 °C under 0.5 mmHg vacuum overnight to remove any traces of water. Toluene, THF, and pentane used in the preparation of **1a**,**b** and **2a**−**c** and in the catalytic hydroarylation reactions were passed through columns of activated alumina (type A2, size 12 × 32, Purify Co.) under nitrogen pressure, sparged with $N_2$, and stored over molecular sieves prior to use. THF-$d_8$ was stirred under nitrogen over sodium/benzophenone ketyl, vacuum-transferred into a sealable storage vessel, degassed using three consecutive freeze−pump−thaw cycles, and stored over activated 3 Å molecular sieves. Toluene-$d_8$ was transferred into a sealable storage vessel, degassed using three consecutive freeze−pump−thaw cycles, and stored over activated 3 Å molecular sieves.

**Phosphinite 1a.** In an inert-atmosphere box, 2,3-dimethylphenol (1.80 mmol, 0.259 g) and 4 mL of THF were added to a glass Kontes vial. NaH (1.98 mmol, 0.0475 g) was added in small portions to the solution. The reaction mixture was stirred for 5 min, and chlorodiisopropylphosphine (1.80 mmol, 0.290 mL) was slowly added. The vial was capped, removed from the inert-atmosphere box, and heated to 100 °C for 14 h. The reaction vessel was returned to the inert-atmosphere box, and the reaction mixture was filtered through basic alumina, with hexanes as eluent. Solvents were evaporated to give 0.35 g of **1a** as a colorless oil (82%). $^1$H NMR (400 MHz, $CDCl_3$): $\delta$ 7.11 (dd, $J$ = 3.7, 8.4 Hz, 1H), 6.92 (t, $J$ = 7.9 Hz, 1H), 6.70 (d, $J$ = 7.3 Hz, 1H), 2.22 (s, 3H), 2.15 (s, 3H), 1.92 (m, 2H), 1.11 (m, 12H). $^{31}$P NMR (162 MHz, $CDCl_3$): $\delta$ 141.45. Anal. Calcd for $C_{14}H_{23}OP$: C, 70.56; H, 9.73. Found: C, 70.35; H, 9.96. GC-MS (*m/z* (% relative intensity, ion)): 238.30 (100, $M^+$), 223.20 (19, M − Me), 195.20 (42, M − *i*-Pr), 151.10 (42, M − *i*-$Pr_2$).

**Phosphinite 1b.** In an inert-atmosphere box, 2,6-dimethylphenol (10.0 mmol, 1.28 g), triethylamine (15.0 mmol, 2.10 mL), and toluene (10 mL) were added to an oven-dried bomb. Chlorodiisopropylphosphine (10.0 mmol, 1.50 g) was added to this solution. The bomb was removed from the inert-atmosphere box and heated at 100 °C for 12 h. In the inert-atmosphere box, the reaction mixture was filtered through basic alumina, with hexanes as eluent, and solvents were removed in vacuo to give 2.20 g of **1b** as a colorless oil (92%). $^1$H NMR (400 MHz, $CDCl_3$): $\delta$ 6.97 (d, $J$ = 7.3, 2H), 6.84 (t, $J$ = 7.5, 1H), 2.35 (s, 6H), 2.00 (m, 2H), 1.14 (m, 12H). $^{31}$P NMR (162 MHz, $CDCl_3$): $\delta$ 155.34. Anal. Calcd for $C_{14}H_{23}OP$: C,

70.56; H, 9.73. Found: C, 70.80; H, 9.95. GC-MS (*m/z* (% relative intensity, ion)): 238.30 (100, $M^+$), 195.20 (53, M − *i*-Pr), 151.10 (56, M − *i*-$Pr_2$).

**General Procedure for the Preparation of Phosphinite Complexes 2a−c.** In an inert-atmosphere box, the appropriate ligand, L (0.200 mmol), was added to an orange solution of **1a** (0.200 mmol, 0.0477 g) and $[RhCl(coe)_2]_2$ (0.100 mmol, 0.0716 g) in 4 mL of toluene in a Kontes vial. The vial was sealed, removed from the inert-atmosphere box, and heated at 45 °C for 6 h. The vial was returned to the box, and the red (**2a** and **2b**) or yellow (**2c**) solution was concentrated to give an orange oil. This oil was dissolved in a minimal volume (ca. 0.5 mL) of toluene, placed in a vial containing ca. 5 mL of pentane, sealed, and allowed to sit at room temperature to give analytically pure solid samples of **2a−c** after filtration and rinsing with pentane.

**$[RhCl(PPh_3)(i\text{-}Pr_2POXy)]_2$ (2a).** Yield: 0.134 g (73%) of light red powder. Anal. Calcd for $C_{64}H_{76}Cl_2O_2P_4Rh_2$: C, 60.15; H, 6.01. Found: C, 60.42; H, 6.09. $^1$H NMR ($d_8$-toluene, 400 MHz): $\delta$ 10.30 (d, $J$ = 8.2, 2H), 8.01 (m, 10H), 7.1−6.9 (m, 24H), 2.11 (m, 4H), 2.01 (s, 6H), 1.79 (s, 6H), 1.15 (m, 12H), 1.05 (m, 12H). $^{31}$P NMR ($d_8$-toluene, 162 MHz): $\delta$ 156.34 (dd, $^1J_{Rh-P}$ = 210.2, $^2J_{P-P}$ = 44.1), 49.76 (dd, $^1J_{Rh-P}$ = 203.4, $^2J_{P-P}$ = 44.4). A small portion of this material was dissolved in toluene with gentle heating (ca. 45 °C) and recrystallized by vapor diffusion of pentane into the toluene solution of the red powder to give dark orange crystals suitable for X-ray analysis.

**$[RhCl(PMe_3)(i\text{-}Pr_2POXy)]_2$ (2b).** Yield: 0.119 g (65%) of red crystals suitable for X-ray analysis. Anal. Calcd for $C_{34}H_{64}Cl_2O_2P_4Rh_2$: C, 45.09; H, 7.14. Found: C, 44.85; H, 7.25. Solution NMR spectra showed a mixture (1.7:1) of two isomers. $^1$H NMR ($d_8$-toluene, 400 MHz): $\delta$ 9.51 (m, $J$ = 8.2 Hz, 2 H), 6.9 (m, 2H), 6.76 (m, 2 H), 2.50 (m, 4 H), 2.13 (m, 12H), 1.81 (m, 7.7H), 1.71 (m, 4.3H), 1.30 (m, 12H), 1.28 (s, 11H), 2.10 (s, 7H). $^{31}$P NMR ($d_8$-toluene, 162 MHz): $\delta$ 171.0 (dd, $^1J_{Rh-P}$ = 226.1, $^2J_{P-P}$ = 50.4), 170.0 (dd, $^1J_{Rh-P}$ = 225.2, $^2J_{P-P}$ = 49.4), 6.73 (dd, $^1J_{Rh-P}$ = 187.6, $^2J_{P-P}$ = 50.4), 6.36 (dd, $^1J_{Rh-P}$ = 188.6, $^2J_{P-P}$ = 50.4).

**$[RhCl(t\text{-}BuNC)(i\text{-}Pr_2POXy)]_2$ (2c).** Yield: 0.067 g (72%) of yellow crystals suitable for X-ray analysis. $^1$H NMR ($d_8$-toluene, 400 MHz): $\delta$ 9.25 (d, $J$ = 8.3, 2H), 7.10 (t, $J$ = 7.8, 2H), 6.71 (d, $J$ = 7.5, 2H), 2.52 (m, 2H), 2.15 (s, 6H), 2.10 (s, 6H), 1.66 (d, $J$ = 7.1, 6H), 1.63 (d, $J$ = 7.1, 6H), 1.54 (d, $J$ = 7.1, 6H), 1.51 (d, $J$ = 7.1, 6H), 0.75 (s, 18H). $^{31}$P NMR ($d_8$-toluene, 162 MHz): $\delta$ 171.66 ppm (d, $^1J_{Rh-P}$ = 215.1). HRMS-EI (*m/z*): $[M]^+$ calcd for $C_{38}H_{64}O_2N_2P_2Cl_2Rh_2$, 918.193; found, 918.195.

**In Situ Analysis of $RhCl(PPh_3)_2(i\text{-}Pr_2POXy)$ (3a).** In an inert-atmosphere box, **2a** (0.006 mmol, 0.0071 g), $PPh_3$ (0.012 mmol, 0.0031 g), and 0.6 mL of $d_8$-toluene were added to a J. Young tube. The tube was sealed, heated to 45 °C, and monitored by NMR spectroscopy. Three major signals were observed by $^{31}$P NMR spectroscopy. $^{31}$P NMR ($d_8$-toluene, 162 MHz): $\delta$ 153.3 (ddd, $^1J_{Rh-P\mathbf{1a}}$ = 163.4, $^2J_{P\mathbf{1a}-PPh_3,trans}$ = 368.6, $^2J_{P\mathbf{1a}-PPh_3,cis}$ = 36.7), 49.4 (dt, $^1J_{Rh-PP}$ = 195.8, $^2J_{P-PPh_3/\mathbf{1a}}$ = 36.5), 27.5 (ddd, $^1J_{Rh-P\mathbf{1a}}$ = 163.4, $^2J_{P\mathbf{1a}-PPh_3,trans}$ = 368.6, $^2J_{P\mathbf{1a}-PPh_3,cis}$ = 36.7).

**Diphenyl (3-Methoxybenzyl)phosphonate.** (3-methoxyphenyl)methanol (0.0580 mol, 7.22 mL), diisopropylethylamine (0.0880 mol, 15.0 mL), DMAP (0.00580 mol, 0.709 g), and 160 mL of $CH_2Cl_2$ (distilled from $CaH_2$ under $N_2$ immediately prior to use) were added to an oven-dried round-bottom flask purged with $N_2$. The solution was cooled to −50 °C, and diphenyl chlorophosphate (0.0880 mol, 18.2 mL) was added dropwise. The reaction mixture was warmed to room temperature and stirred for 22 h. A saturated solution of $NH_4Cl$ was added to the reaction mixture, the layers were separated, and the aqueous layer was extracted with three portions of $CH_2Cl_2$. The combined organic layers were washed with brine and dried with $Na_2SO_4$, and solvents were evaporated in vacuo. The residue was purified by column chromatography ($SiO_2$, 1/4 EtOAc/hexanes) to give 19.7 g of the desired phosphate as a colorless oil (92%). $^1$H NMR (400 MHz, $CDCl_3$): $\delta$ 7.33 (t, $J$ = 7.9, 4H), 7.27 (dt, $J$ = 2.4, 6.8, 1H), 7.20 (m, 6H), 6.94 (d, $J$ = 7.9, 1H), 6.89 (m, 2H), 5.25 (d, $J$ = 8.6, 2H), 3.76 (s, 3H). $^{13}$C NMR (101 MHz, $CDCl_3$): $\delta$ 159.75, 156.21, 153.84, 150.43, 136.64, 129.75, 125.34, 120.09, 114.63, 113.07, 70.49, 55.20. $^{31}$P NMR (162 MHz, $CDCl_3$): $\delta$ −11.82. HRMS-EI (*m/z*): $[M]^+$ calcd for $C_{20}H_{19}O_5P$, 370.0970; found, 370.0972.

**1-(2,2-Dimethylbut-3-enyl)-3-methoxybenzene.** A stir bar, 100 mL of THF (distilled from Na/benzophenone ketyl under $N_2$ immediately prior to use), and magnesium (1.17 mol, 28.3 g, ground in a mortar and pestle immediately prior to use) were placed in an oven-dried, three-necked round-bottom flask purged with $N_2$. 1-Chloro-3-methyl-2-butene (0.146 mol, 16.4 mL) and 100 mL of THF were added to an addition funnel attached to the center neck of the reaction flask. The Mg suspension was cooled to −30 °C, and the alkene solution was slowly added dropwise. The reaction mixture was warmed to room temperature and was stirred for 3 h. Diphenyl (3-methoxybenzyl)phosphonate (0.0600 mol, 22.2 g) and THF (100 mL) were placed in another oven-dried round-bottom flask equipped with a stir bar under nitrogen. This solution was cooled to −40 °C, and the Grignard solution (titrated to 0.6 M immediately before use) was transferred dropwise via cannula. The reaction mixture was warmed to room temperature and stirred for 16 h. Saturated $NH_4Cl$ was added slowly to the reaction mixture, and the aqueous layer was extracted with EtOAc. The combined organic layers were washed with brine and dried with $MgSO_4$, and the solvents were removed in vacuo. The residue was purified by column chromatography ($SiO_2$, 100% hexanes) to give 11.4 g of the desired product as a colorless oil (82.0%). $^1$H NMR (400 MHz, $CDCl_3$): $\delta$ 7.20 (t, $J$ = 7.8 Hz, 1H), 6.75 (m, 3H), 5.90 (dd, $J$ = 10.8, 17.7 Hz, 1H), 4.93 (m, 2H), 3.82 (s, 3H), 2.59 (s, 2H), 1.04 (s, 6H). $^{13}$C NMR (101 MHz, $CDCl_3$): $\delta$ 158.93, 148.11, 140.42, 128.39, 123.16, 116.50, 111.02, 110.50, 55.08, 49.11, 37.63, 26.52. HRMS-EI (*m/z*): $[M]^+$ calcd for $C_{13}H_{18}O$, 190.1358; found, 190.1358.

**3-(2,2-Dimethylbut-3-enyl)phenol.** A 60% dispersion of sodium hydride in mineral oil (65.0 mmol, 2.62 g) was placed in an oven-dried round-bottom flask. The flask was fitted with a condenser, the apparatus was purged with $N_2$, and 60 mL of DMF (anhydrous, Acros) was added. The suspension was cooled to 0 °C with stirring. Ethanethiol (62.5 mmol, 4.6 mL) was slowly added to the suspension through the condenser to control the vigorous reaction that occurs upon addition. Once the reaction subsided, the reaction mixture was heated to 110 °C to give a brown solution. A solution of 1-(2,2-dimethylbut-3-enyl)-3-methoxybenzene (25.0 mmol, 4.78 g) in 30 mL of DMF (combined directly into a syringe) was slowly added to the reaction mixture (through the condenser). An additional 30 mL of DMF was added through the condenser, and the mixture was heated at 110 °C for 16 h. The mixture was cooled to room temperature, and water (250 mL) was added. The layers were separated, and the aqueous layer was extracted with EtOAc (3 × 50 mL). The combined organic layers were washed with brine and dried with $MgSO_4$, and the solvents were removed in vacuo. The resulting oil was purified by column chromatography ($SiO_2$, 5% EtOAc/hexanes) to give 3.60 g of the desired product as a colorless oil, which solidified after refrigeration (81%). $^1$H NMR (400 MHz, $CDCl_3$): $\delta$ 7.15 (t, $J$ = 7.9, 1H), 6.72 (m, 2H), 6.67 (m, 1H), 5.88 (dd, $J$ = 10.7, 15.5, 1H), 5.36 (s, 1H), 4.92 (m, 2H), 2.56 (s, 2H), 1.03 (s, 6H). $^{13}$C NMR (101 MHz, $CDCl_3$): $\delta$ 154.63, 148.04, 140.81, 128.69, 123.37, 117.57, 112.90, 110.58, 48.91, 37.61, 26.51. HRMS-EI (*m/z*): $[M]^+$ calcd for $C_{12}H_{16}O$, 176.1201; found, 176.1202.

**6,6-Dimethyl-5,6,7,8-tetrahydronaphthalen-1-ol.** In an oven-dried bomb, 3-(2,2-dimethyl-but-3-enyl)phenol (1.08 mmol, 0.190 g), Wilkinson's catalyst (0.0108 mmol, 0.0102 g), *i*$Pr_2$POXy (0.108 mmol, 0.0331 g), and toluene (10.8 mL) were added. The vessel was sealed, removed from the inert-atmosphere box,

and heated at 130 °C for 17 h. The solution was diluted with toluene (10 mL) and transferred to a round-bottom flask. To this was added 1 M HCl (10−15 mL), and the mixture was stirred vigorously for 50 min. The layers were separated, and the aqueous layer was extracted with EtOAc. The combined organic layers were washed with brine and dried with $MgSO_4$, and the solvents were evaporated in vacuo. The residue was purified by column chromatography ($SiO_2$, 5% EtOAc/hexanes) to give 0.15 g of the desired product as a yellow oil (80%). $^1$H NMR (400 MHz, $CDCl_3$): $\delta$ 7.05 (t, $J$ = 8.1, 1H), 6.71 (d, $J$ = 8.1, 1H), 6.66 (d, $J$ = 8.1, 1H), 4.75 (s, 1H), 2.70 (t, $J$ = 6.8, 2H), 2.58 (s, 2H), 1.65 (t, $J$ = 6.8, 2H), 1.03 (s, 6H). $^{13}$C NMR (101 MHz, $CDCl_3$): $\delta$ 153.35, 138.35, 126.27, 122.00, 122.07, 111.82, 43.48, 35.34, 29.18, 27.90, 20.51. HRMS-EI (*m/z*): $[M]^+$ calcd for $C_{12}H_{16}O$, 176.1201; found, 176.1201.

**6-(3,3-Dimethylbutyl)-2,3-dimethylphenol.** In an inert-atmosphere box, 2,3-dimethylphenol (1.39 mmol, 0.170 g), *i*-$Pr_2POXy$ (0.139 mmol, 0.0355 g), 3,3-dimethyl-1-butene (6.95 mmol, 0.896 mL), Wilkinson's catalyst (0.0695 mmol, 0.0643 g), and toluene (13.9 mL) were placed in an oven-dried bomb equipped with a stir bar. The bomb was sealed, brought out of the inert-atmosphere box, and heated to 135 °C, and the reaction mixture was stirred for 17 h. The reaction mixture was transferred to a 50 mL round-bottom flask with toluene. An aqueous solution of HCl (1 M, 15−25 mL) was added, and the solution was stirred vigorously for 1 h. The layers were separated, and the aqueous layer was extracted with EtOAc. The organic layers were combined, washed with brine, dried with $MgSO_4$, and concentrated in vacuo. The residue was purified by column chromatography ($SiO_2$, 5% EtOAc/hexanes) to give 0.21 g of the desired product (72%). $^1$H NMR (400 MHz, $CDCl_3$): $\delta$ 6.88 (d, $J$ = 7.7, 1H), 6.71 (d, $J$ = 7.6, 1H), 2.53 (m, 2H), 2.26 (s, 3H), 2.18 (s, 3H), 1.48 (m, 2H), 0.99 (s, 9H). HRMS-EI (*m/z*): $[M]^+$ calcd for $C_{14}H_{22}O$, 206.1671; found, 206.1674.

**Typical Procedure for NMR-Tube Reactions.** In an inert-atmosphere box, 2,3-dimethylphenol, complex **2a**, and phosphinite **1b** were rinsed into an oven-dried, medium-walled NMR tube using 2 × 0.2 mL of $d_8$-toluene. Neohexene was added to the tube via syringe, and an additional 0.2 mL of $d_8$-toluene was used to rinse the residue from the reagent vials and neohexene down the NMR tube. The tube was fitted with a Cajon adapter, removed from the inert-atmosphere box, attached to a vacuum line, and flame-sealed. The tube was heated at 135 °C, and the reaction was monitored by NMR spectroscopy, which showed 88% conversion to 6-(3,3-dimethylbutyl)-2,3-dimethylphenol after 2.8 h. This result matched those obtained using the aforementioned screening conditions (Table 4, entry 3). Essentially the same procedure was used for all reactions described in the text, with substitutions for alternative reagents.

**Procedure for Incorporation of D into 1a.** In an inert-atmosphere box, **1a** (0.28 mmol, 0.67 g), **2a** (0.0070 mmol, 0.0090 g), and toluene (2.8 mL) were added to an oven-dried Kontes reaction vessel equipped with a Teflon stopper. The tube was sealed, removed from the box, degassed using three freeze−pump−thaw cycles, and charged with ca. 0.8 atm of $D_2$ gas. The tube was again sealed and heated in an oil bath at 105 °C for 10 h. The reaction mixture was then transferred to a vial and stirred vigorously with 5 mL of 1 M HCl for 1 h. The organic layer was separated, and the aqueous layer was extracted with 2 × 10 mL of $Et_2O$. The combined organics were washed with 10 mL of brine, dried over $Na_2SO_4$, and concentrated to give a brown oil. The oil was purified by column chromatography ($SiO_2$, 10% EtOAc/hexanes) to give 0.022 g of 2,3-dimethylphenol (63%) as a white solid. $^1$H NMR showed 75% incorporation of deuterium at the ortho position and no incorporation of D at any other site in the molecule relative to the meta methyl group, which was used as an internal standard. $^1$H NMR (400 MHz, $CDCl_3$): $\delta$ 6.96 (m, 1H), 6.60 (d, $J$ = 7.57, 1H), 6.35 (d, $J$ = 8.04, 0.25H), 2.28 (s, 3H), 2.17 (s, 3H).

**Computational Details.** DFT geometry optimization and $^1$H NMR chemical shielding calculations of model complex **4** were performed using the program Gaussian03 at the mPW1PW91/SDD level of theory, as described elsewhere.[22] DFT geometry optimization and single point calculations for *cis*-**5a**, *cis*-**5c**, *cis*-**5e**, and *trans*-**5a**−**e** were performed using the program Jaguar at the B3LYP,LACVP**++ level of theory as described elsewhere.[23] Geometry optimization of *cis*-**5b** and *cis*-**5d** was performed at the B3LYP, LACVP++ level of theory, while the single-point calculations for these structures were carried out at the B3LYP, LACVP**++ level of theory.

**X-ray Structure Determinations. General Considerations.** X-ray crystal structures were obtained by Drs. Fredrick Hollander and Allan Oliver at the UCB X-ray facility (CHEXRAY). Crystals were mounted on glass fibers using Paratone N hydrocarbon oil. All measurements were made on a SMART[24] CCD area detector with graphite-monochromated Mo Kα radiation. Data were integrated by the program SAINT[25] and were corrected for Lorentz and polarization effects. Data were analyzed for agreement and possible absorption using XPREP.[26] The structures were solved by direct methods[27] and expanded using Fourier techniques.[27] Crystal data and structure refinement details for **2a**−**c** are given in Table 2.

**Acknowledgment.** This work was supported by NIH Grant No. GM069559 (to J.A.E.) and by the Director, Office of Energy Research, Office of Basic Energy Sciences, Chemical Sciences Division, U. S. Department of Energy, under Contract No. DE-AC02-05CH11231 (to R.G.B.). J.W. is funded by a Jean Dreyfus Boussevain Award. All calculations were conducted on the UCB Molecular Graphics and Computation Facility computer cluster supported by NSF Grant No. CHE-0233882. This work could not have been completed without many helpful discussions with Dr. Jennifer R. Krumper. Thanks also to Dr. Fredrick J. Hollander and Dr. Allen G. Oliver at the UCB X-ray diffraction facility (CHEXRAY) for solving the structures of **2a**−**c**, Dr. Yong Zhang and Prof. Eric Oldfield for geometry optimization and calculated NMR chemical shifts of **4**, and Kathy Durkin and Dr. Nate Crawford for help with DFT calculations for **5a**−**e**.

**Supporting Information Available:** CIF files giving X-ray structure data for **2a**−**c**, tables giving Cartesian coordinates for **3**, *cis*-**5a**−**e**, and *trans*-**5a**−**e**, and text giving the complete Gaussian reference. This material is available free of charge via the Internet at http://pubs.acs.org.

OM050700I

(22) (a) Pople, J. A. et al. Gaussian 03; Gaussian, Inc., Pittsburgh, PA, 2003. (b) Godbout, N.; Havlin, R.; Salzmann, R.; Debrunner, P. G.; Oldfield, E. *J. Phys. Chem. A* **1998**, *102*, 2342−2350. (c) Zhang, Y.; Guo, Z.; You, X.-Z. *J. Am. Chem. Soc.* **2001**, *123*, 9378−9387.

(23) Tan, K. L.; Bergman, R. G.; Ellman, J. A. *J. Am. Chem. Soc.* **2002**, *124*, 3202−3203.

(24) Area-Detector Software Package; Siemens Industrial Automation, Inc., Madison, WI, 1995.

(25) SAX Area-Detector Integration Program, version 4.024; Siemens Industrial Automation, Inc., Madison, WI, 1995.

(26) XPREP, version 5.03, part of the SHELXTL Crystal Structure Determination Package; Siemens Industrial Automation, Inc., Madison, WI, 1995.

(27) Beurskens, P. T.; Admiraal, G.; Beurskens, G.; Bosman, W. P.; de Gelder, R.; Israel, R.; Smits, J. M. M. The DIRDIF-94 Program System; Technical Report of the Crystallography Laboratory; University of Nijmegen, Nijmegen, The Netherlands, 1994.